The effects of PbZn 1/3 Nb 2/3 O 3 -doping on structural, thermal, optical, dielectric, and ferroelectric properties of BaTiO 3 ceramics

J. Suchanicz, K. Świerczek, D. Sitko, P. Czaja, Pascal Marchet, H. Czternastek, D. Majda

The effects of $PbZn_{1/3}Nb_{2/3}O_3$-doping on structural, thermal, optical, dielectric, and ferroelectric properties of $BaTiO_3$ ceramics

J. Suchanicz, K. Świerczek, D. Sitko, P. Czaja, P. Marchet, H. Czternastek, and D. Majda

Citation: Journal of Applied Physics **122**, 124105 (2017); doi: 10.1063/1.5005516
View online: http://dx.doi.org/10.1063/1.5005516
View Table of Contents: http://aip.scitation.org/toc/jap/122/12
Published by the American Institute of Physics

The effects of $PbZn_{1/3}Nb_{2/3}O_3$-doping on structural, thermal, optical, dielectric, and ferroelectric properties of $BaTiO_3$ ceramics

J. Suchanicz,[1,a)] K. Świerczek,[2] D. Sitko,[3] P. Czaja,[1] P. Marchet,[4] H. Czternastek,[3] and D. Majda[5]

[1]*Institute of Technology, Pedagogical University, ul. Podchorazych 2, 30-084 Krakow, Poland*
[2]*AGH University of Science and Technology, Faculty of Energy and Fuels, Department of Hydrogen Energy, al. Mickiewicza 30, 30-059 Krakow, Poland*
[3]*Institute of Physics, Pedagogical University, ul. Podchorazych 2, 30-084 Krakow, Poland*
[4]*CNRS Université de Limoges, Science des Procédés Céramiques et de Traitementts de Surface, Centre Européen de la Céramique, Limoges Cedex, France*
[5]*Faculty of Chemistry, Jagiellonian University, ul.Ingardena 3, 30-060 Krakow, Poland*

(Received 7 April 2017; accepted 17 September 2017; published online 29 September 2017)

Low-lead (1-x)BT-xPZN (x = 0, 0.025, 0.05, 0.075, 0.10, 0.125, and 0.15) ceramics were successfully synthesized by the spark-plasma-sintering method for the first time. Their phase transition behavior as well as structural, thermal, optical, and electrical properties was investigated. These materials exhibit the structure of perovskite-type solid solutions and undergo a sequence of phase transitions, typical of pure $BaTiO_3$ (BT). The dielectric test results revealed that with the increase in the $PbZn_{1/3}Nb_{2/3}O_3$ (PZN) content, the frequency dispersion of electric permittivity increases, whilst the dielectric/ferroelectric properties tend to deteriorate, which is characteristic of relaxor-type behavior. Therefore, it is reasonable to suppose that these ceramics progressively lack long-range ordering. These effects are due to the competition between lone-pair electrons' induced changes in the A-O band upon Pb^{2+} addition and ionic size differences. In general, the transition temperatures observed by dielectric analyses are in good agreement with those obtained from X-ray diffraction and differential scanning calorimetry measurements. The BT-PZN system may help to understand why relaxor behavior appears in perovskite-based materials. It appears that these materials can become a good starting point for the development of new low-lead electronic ceramics. *Published by AIP Publishing*. https://doi.org/10.1063/1.5005516

I. INTRODUCTION

Ferroelectric ceramics with a perovskite structure are an excellent choice for applications in electronic devices such as transducers, actuators, and sensors;[1] $BaTiO_3$ (BT) and $PbZn_{1/3}Nb_{2/3}O_3$ (PZN) seem to be most promising due to their excellent electrical properties.[2,3]

BT undergoes three phase transitions: rhombohedral-orthorhombic transition (R3m-Amm2) at about −90 °C, orthorhombic-tetragonal transition (Amm2-P4 mm) at about 5 °C, and tetragonal-cubic transition (P4 mm-Pm3m) at about 120 °C.[4] The cubic phase is paraelectric, while the others are ferroelectric. BT was believed to be a displacive-type ferroelectric material although some experimental results would suggest an order-disorder mechanism.[5–8] It was also postulated that the fluctuating spontaneous polarization originates from the presence of an electric dipole induced by hopping of the Ti cation around its equilibrium position at temperatures far above T_c, similar to relaxor ferroelectrics.[9] However, the role and nature of displacive and order-disorder components during the phase transitions have not been fully understood or adequately described yet. Similar to PMN, PZN is a relaxor and it displays cubic symmetry at high temperatures. Unlike PMN, however, PZN reveals a macroscopic lattice distortion with rhombohedral symmetry at room temperature. A structural phase transition from cubic (Pm3m) to rhombohedral (R3m) takes places at around 140 °C.[10,11] However, some experimental results point to the presence of two kinds of local symmetries: the B-site chemical disorder and the off-axis shift of lead ions.[11] Thus, PZN can be classified as a disordered and inhomogeneous material.

With regard to complementary features of BT and PZN reported in numerous publications, the solid solution BT-PZN is expected to combine the properties of both normal ferroelectric and relaxor ferroelectrics and to exhibit better properties than single-phase BT and PZN. It is extremely difficult to prepare pure polycrystalline PZN by the conventional mixed-oxide route because of an unwanted pyrochlore-type phase, highly detrimental to the electrical properties. However, mixing PZN with BT is expected to yield a pure perovskite structure without the presence of an undesirable pyrochlore phase.

With these considerations in mind, we have undertaken the synthesis of (1-x)BT-xPZN systems (x = 0, 0.025, 0.05, 0.075, 0.1, 0.125, and 0.15) to produce and thoroughly investigate their structural, thermal, optical, dielectric, and ferroelectric properties to get a better insight into various aspects of their behavior.

II. EXPERIMENTAL DETAILS

In the first stage, good quality of BT-PZN ceramics had to be obtained by the conventional sintering method.

a)Author to whom correspondence should be addressed: sfsuchan@up.krakow.pl

Unfortunately, the samples obtained in this way were rather fragile, with density below 88% of the theoretical value and low resistivity, and therefore, the next sample was obtained by the Spark Plasma Sintering (SPS) route.

The materials were sintered using Spark Plasma Sintering (SPS) equipment (FCT system, Germany). The powders (without a plasticizer) of basic oxides $BaCO_3$, TiO_2, Nb_2O_5, PbO, and ZnO were placed in a graphite die (inner diameter of 20 mm) and uniaxially pressed at 35 MPa. They were then heated up to 1190–1210 °C with a heating rate of 100 °C/min. They were sintered at the final temperature for 5 min. After the sintering process, the samples were first allowed to cool within the matrix and then removed. The entire SPS process took place in the protective Ar atmosphere. After SPS sintering, the sample was annealed at 1000 °C for 2 h in air to remove the carbon contamination. Samples obtained in this way have revealed a pure perovskite phase with a relative density above 96%.

Structural tests were performed by the X-ray diffraction (XRD) method. Measurements of the synthesized materials were taken using a Panalytical Empyrean diffractometer in the 10°–110° range with CuK_α radiation. For high-temperature measurements (from 30 °C to 300 °C), the diffractometer was equipped with an Anton Paar HTK 1200N oven-chamber. In the low temperature range (−250 °C to 20 °C), an Oxford cryostat was mounted and evacuated using rotary and turbomolecular pumps. Rietveld analysis of the XRD data was supported by GSAS/EXPGUI software.[12,13] For clarity, the results shown in the respective figures were numerically stripped of the $K_{\alpha 2}$ component by the Rachinger method.

The microstructure of the synthesized ceramics was analysed using a Model Hitachi S4700 scanning microscope, with field emission and a Noran Vantage EDS system.

The specific heat measurements were performed by differential scanning calorimetry (DSC) using a Netzsch F3 Maia scanning calorimeter in the temperature range of −150 °C to 300 °C under an argon atmosphere, at a flow rate of 30 ml/min. The specimen consisting of a single piece of material with an average mass of 20 mg was placed in an alumina crucible. Measurement data were collected upon heating and cooling with a constant rate of 10 °C/min.

Raman spectra were recorded using a Bio-Rad FTS 6000 spectrometer with an Nd-Yag laser system, where the 1064 nm line was used as the excitation line. The laser power was 200 mW, and the spectra were collected with a resolution of 4 cm^{-1}.

The dielectric measurements were carried out for silver electrode samples using a GW 821 LCR meter in the

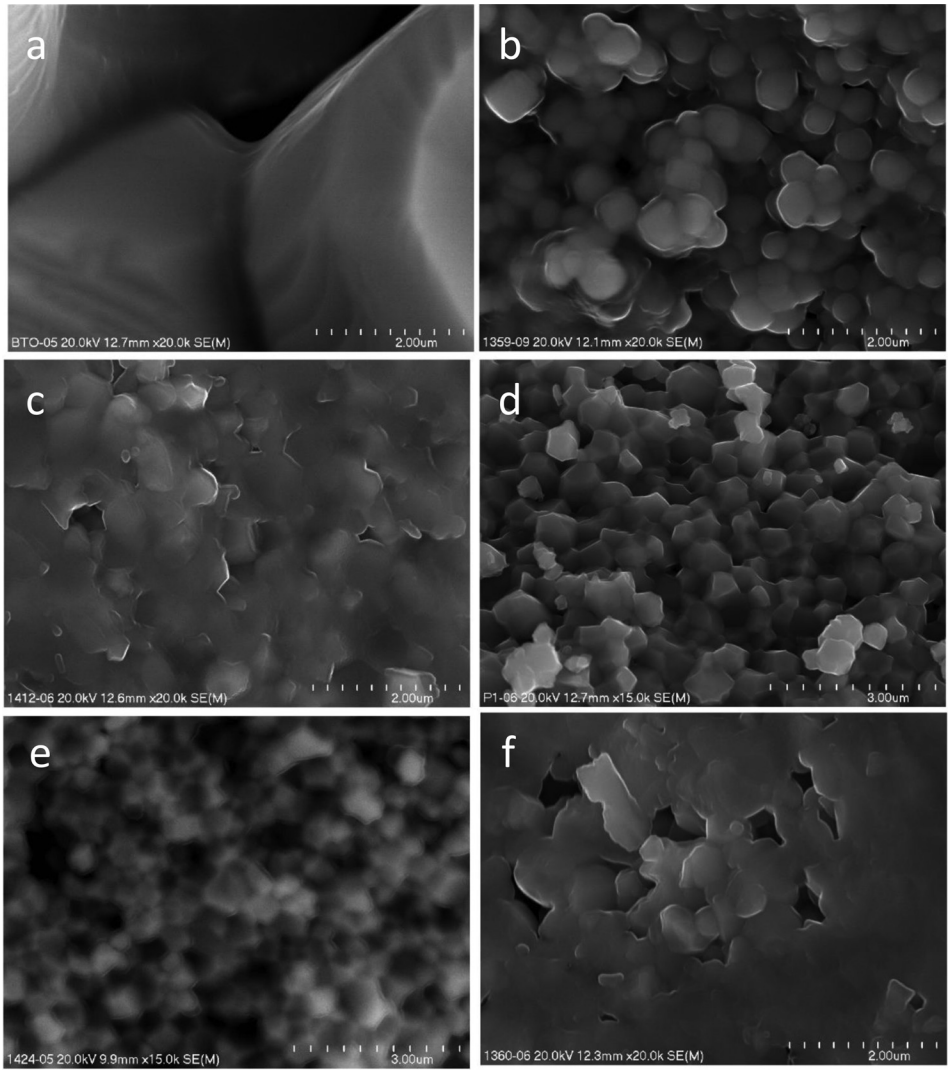

FIG. 1. SEM micrograph of the fracture surface of (1-x)BT-xPZN ceramics: x = 0 (a), x = 0.025 (b), x = 0.05 (c), x = 0.075 (d), x = 0.1 (e), and x = 0.125 (f).

temperature and frequency ranges of room temperature to 300 °C and 20 Hz to 2 MHz, respectively, and under the applied electric field of 20 V cm^{-1}. The data were collected with a step of 0.1 °C upon heating and cooling, with the temperature varying at a rate of 100 °C/h, and using an automatic temperature controller.

The pyroelectric current was recorded by a quasistatic method at the rate of 10 °C/min. The polarizing procedure was applied in the temperature range of 170 °C down to room temperature, under a dc electric field of 5 kV/cm.

III. RESULTS AND DISCUSSION

Well-developed grains with an average grain size of 6 μm were observed for BT, as shown in Fig. 1(a). A decrease in the average grain size to 0.1–0.8 μm was observed for BT-PZN [Figs. 1(b)–1(d)]. EDS analysis confirmed the high purity and specified chemical composition of the samples.

All investigated BT-PZN samples with a doping level of up to 15 at. % were found to be single phase. Figures 2(a)–2(f) show a selected range of diffractograms recorded

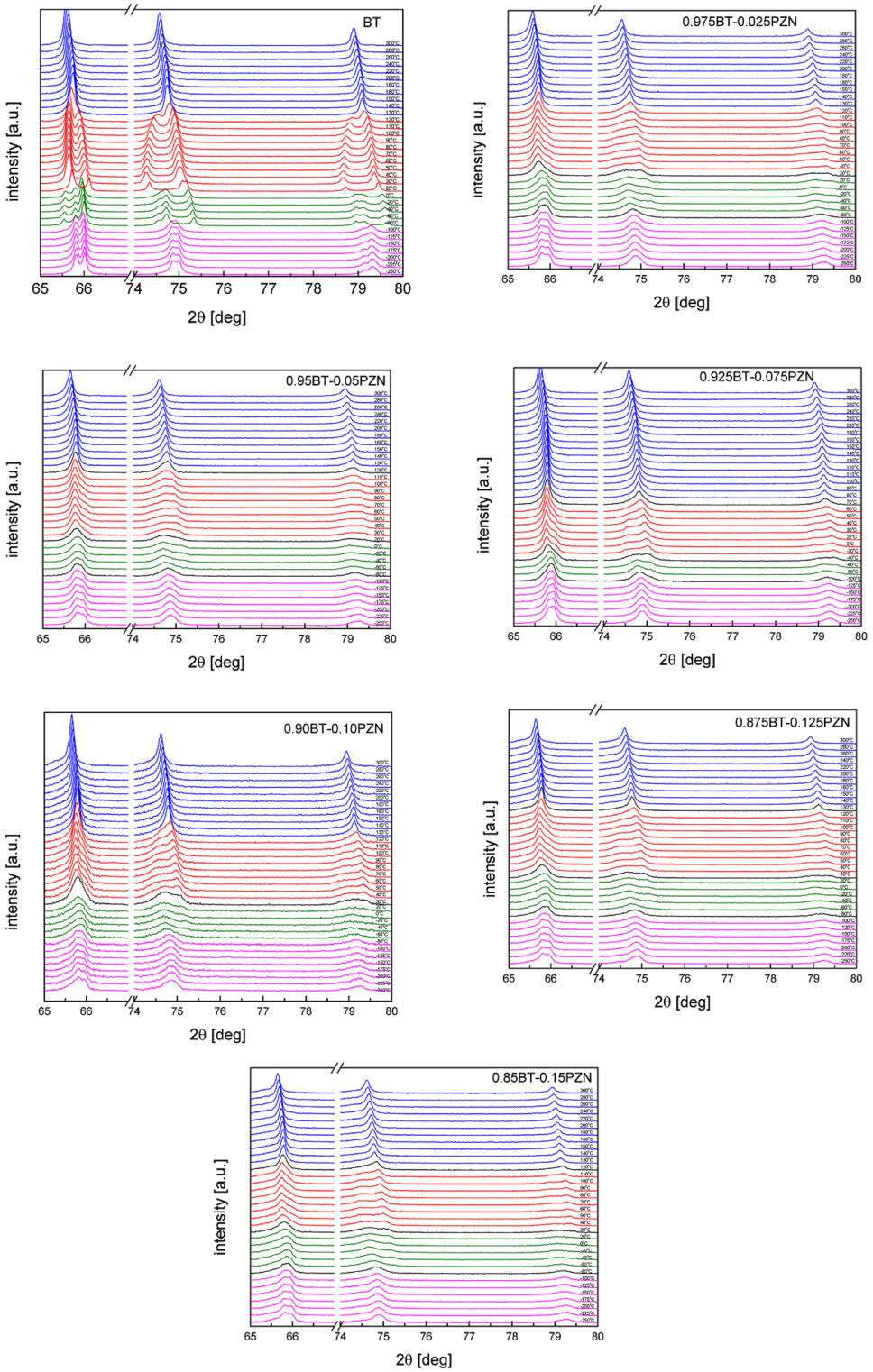

FIG. 2. Selected range of XRD data of (1-x)BT-xPZN ceramics: x = 0 (a), x = 0.025 (b), x = 0.05 (c), x = 0.075 (d), x = 0.1 (e), x = 0.125 (f), and x = 0.15 (g). Different colors designate the temperature range where cubic (blue), tetragonal (red), orthorhombic (green), and rhombohedral (magenta) phases are present.

for the investigated compounds in the temperature range of −250 °C up to 300 °C. Structural transformations occurring with the temperature change are observed for all investigated materials. Note that respective phases are indicated with different colors.

Compared to the undoped $BaTiO_3$ perovskite, the recorded structural transitions of BT-PZN 2.5 at. % are not so well defined, revealing broader peaks indicating disordering in the crystal structure. Moreover, no significant changes in temperatures at which the respective transitions occur could be noticed (Fig. 3). In fact, the transition temperatures cannot be accurately determined because of the presence of relatively broad peaks. Essentially, the same behavior was observed for BT-PZN 5 at. %, with virtually no changes in the nature of the recorded diffractograms. Interestingly, in the case of the PZN sample doped with 7.5 at. %, structural transformations were shifted to the lower temperature range, for example, the cubic structure was found to be stable down to 60 °C. As regards materials with a higher PZN content (up to 15 at. %), the respective structural transitions were observed for less-doped compounds, but the actual cause for this behavior of BT-PZN 7.5 at. % oxide is still unclear.

Generally, it can be summarized that the effects of PZN and PMN dopants on host BT are different. In previous works, we reported that PMN reduces the structural distortions of barium titanate, with the cubic phase becoming stable down to lower temperatures, and causes the disappearance of the orthorhombic phase for a doping level of 7.5%.[14] For the PZN dopant, all transitions (cubic–tetragonal–orthorhombic–rhombohedral) in the doped BT are observed up to the doping limit. However, the observed distortions are significantly smaller in magnitude.

Measurements of dielectric properties reveal that BT-PZN ceramics undergo a sequence of phase transitions which are the same as those for pure BT (Fig. 4). The ε(T) peaks first shift towards the higher and then to the lower temperature range. These phase transitions seem to be of first-order with diffused characteristics [inset in Fig. 4(d)]. Dielectric dispersion increases with the increasing PZN content (except for samples with x = 0.075 and 0.125). In addition, samples with x = 0.10 exhibits the relaxor-type behavior [Fig. 4(e)]. The T_m(f) dependence obeys the Vogel-Fulcher (V-F) law

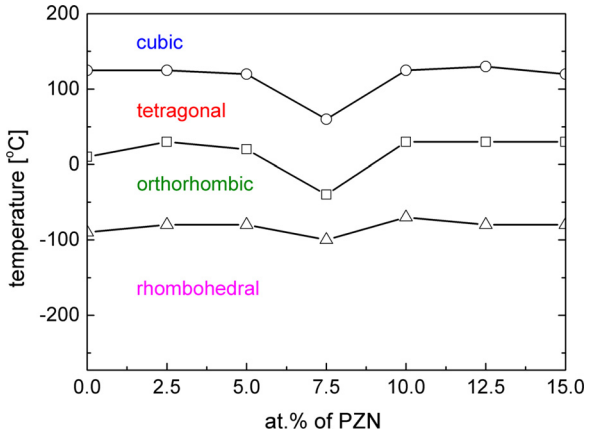

FIG. 3. Phase diagram of (1-x)BT-xPZN ceramics.

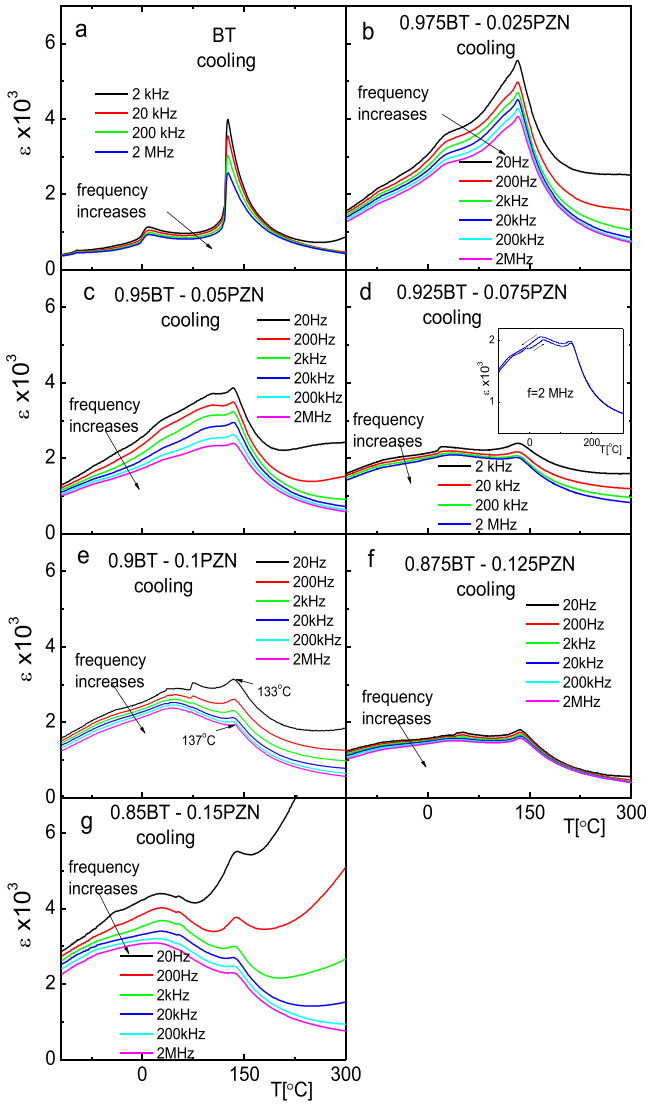

FIG. 4. Temperature dependence of the electric permittivity ε of (1-x)BT-xPZN ceramics on cooling.

with the following parameters: attempt frequency $f_0 = 4.2 \times 10^{14}$ Hz, with a very low activation energy of $E_a = 0.08$ eV, and freezing temperature $T_{VF} = 129$ °C. So, the low value of E_a points to a complex system, with a kind of long-range interaction. The fulfillment of the V-F law may point to the glassy behavior of the material although it does not necessarily imply that complete "freezing" takes place in the system. This issue cannot be fully explained yet because of the narrow frequency band.

Figure 5 shows the temperature dependence of heat flow on the cooling process of the investigated ceramics. The DSC curve for BT reveals three λ-shaped peaks associated with phase transitions. The DSC peaks related to the phase transitions in pure BT become smaller and broader with the increasing PZN content (the calculated latent heats decrease, and the temperature width of the phase transitions, from the beginning to end of the DSC peaks, will increase). Simultaneously, these peaks first shift to the higher and then to the lower temperature range. The broadening of the DSC peaks is related to an increase in the degree of A and B-site

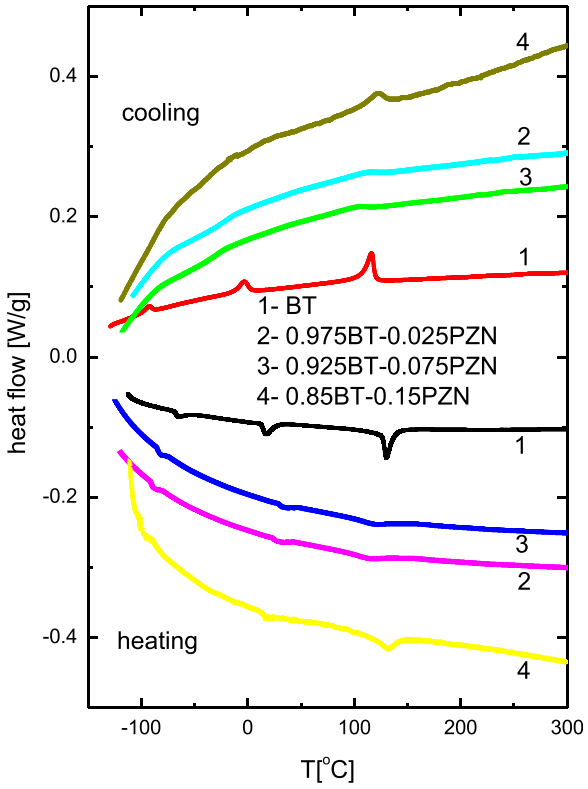

FIG. 5. Temperature evolution of the heat flow of (1-x)BT-xPZN ceramics.

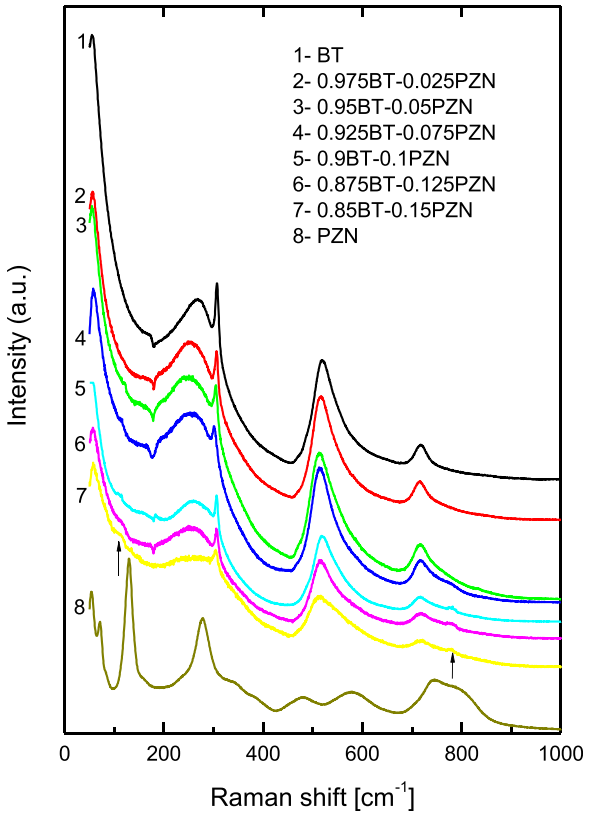

FIG. 6. Room temperature Raman spectra of (1-x)BT-xPZN ceramics.

disorder due to the presence of Pb^{2+} and $(Zn,Nb)^{4+}$ ions. The DSC results imply a very similar evolution of the phase transitions to that observed from X-ray and dielectric analyses.

There may be two reasons why the patterns of Curie temperature changes in the investigated materials are so irregular. The first reason is the higher value of the Curie temperature of PZN (at about 140 °C) in comparison with BT (at about 120 °C), causing T_c to be shifted towards the higher temperature range in the BT-PZN system. The second reason may be a significant decrease in the grain size, causing T_c to shift towards the lower temperature range. An irregular pattern of T_c changes may be attributed to the "competition" between these two effects.

In the cubic phase of BT (space group $O^1{}_h$ (Pm3m)), there are 12 optical modes, which transform the irreducible representation of the point group O_h to $3T_{1u}+T_{2u}$. In the tetragonal phase (space group $C^1{}_{4\nu}$ (P4 mm)), each T_{1u} mode is expected to split into two further modes, transforming as the A_1+E irreducible representation of the point group $C_{4\nu}$. Both A_1 and E modes are Raman active. The T_{2u} silent mode splits into B_1+E modes that are also Raman active.[15,16]

Raman spectra of BT, PZN, and (1-x)BT-xPZN are shown in Fig. 6. A sharp band at around 310 cm^{-1} and a broad band at around 720 m^{-1} (attributed to the E(LO) mode) for BT are characteristic of the tetragonal phase. 272 cm^{-1} and 520 cm^{-1} broad bands are associated with the A_1(LO) mode. A dip at about 180 cm^{-1} is an interference effect due to coupling between A_1 phonons. ~180 cm^{-1}, ~310 cm^{-1}, and ~720 cm^{-1} peaks are generally regarded as indicators of the ferroelectric phase in BT. Thus, it is evident (see Fig. 6) that BT is in its tetragonal ferroelectric phase. Similar bands in the BT ceramic were observed by Fahri *et al.*[16] and by Mao *et al.*[17] The Raman spectra of PZN consist of a number of broad, overlapping lines. The modes of PZN are registered mainly at about 68, 130, 278, 479, 578, 745, and 780 cm^{-1}. Similar bands for PZN were observed by Janolin *et al.*[18] The high-frequency modes above 700 cm^{-1} in perovskites may be attributed to vibrations resulting from the shift of oxygen and also correlated with oxygen vacancies.[19]

Raman spectra of BT and PZN-doped BT are similar to each other, but very different from those of pure PZN. However, the analysis of Fig. 6 reveals that these spectra tend to evolve as the actual composition is varied:

(1) In the first place, more bands become broadened, which indicates that the structure becomes more disordered. This is associated mostly with disorder created at the A and B-sites of BT as a consequence of Pb and Zn/Nb substitution, respectively.
(2) In addition, many of the bands are shifted towards the lower frequency range than for BT. This could be explained by the difference in the mass of Ba and Pb (the Pb mass is far larger than the Ba mass) and between the mass of Ti and Zn/Nb (the Zn/Nb mass is larger than the Ti mass). The band at about 272 cm^{-1} decreases in intensity and moves to the low frequency range, whereas the band at about 310 cm^{-1} decreases in intensity and slightly shifts to lower frequencies. In addition, a new line appears (already visible at about 117 cm^{-1} for 0.95BT-0.05PZN, indicated by an

arrow), which may be evidence of a structural change associated with the A-site symmetry change. The dip at about 180 cm^{-1} has a constant frequency for all compositions. The band at about 520 cm^{-1} decreases in intensity, slightly broadens, and appears to be fixed, which is probable due to a change in the average ion radius in the A and B-sites. The band at about 720 cm^{-1} is also affected, which decreases in intensity and broadens. In addition, another weak mode appears as a shoulder at the higher side of this mode (indicated by an arrow), which is close to the broad band characteristic of PZN centered at around 780 cm^{-1}. These changes can be attributed to the influence of A-site and B-site substitution on oxygen vibrations in TiO_6 and to changes in vacancy concentrations. Decreased intensity and broadening of ~180 cm^{-1}, ~310 cm^{-1}, and ~720 cm^{-1} modes (all of which belong to the ferroelectric state of BT) with the increasing PZN content indicate that the material gradually loses its long-range ferroelectric properties.

The remnant polarization P_r decreases (ferroelectric properties deteriorate) after the incorporation of PZN into BT [Fig. 7(a)], as shown by Raman analyses. P_r is retained in a wide temperature range above the Curie temperature T_c [Fig. 7(a)], and another small anomaly is revealed alongside the main peak in the pyroelectric current $i_p(T)$ [indicated by an arrow in Fig. 7(b)]. This is attributable to the existence of polar regions above T_c. A small anomaly of $i_p(T)$ is also registered for pure BT [Fig. 7(b)]. Zalar *et al.*[20] proved that in BT above T_c (even up to 170–180 °C), there is a tetragonal distortion of the unit cells, or more specifically, there are some polar regions of tetragonal symmetry in the cubic matrix. This temperature range corresponds well to that in which a pyroelectric current anomaly has been observed.

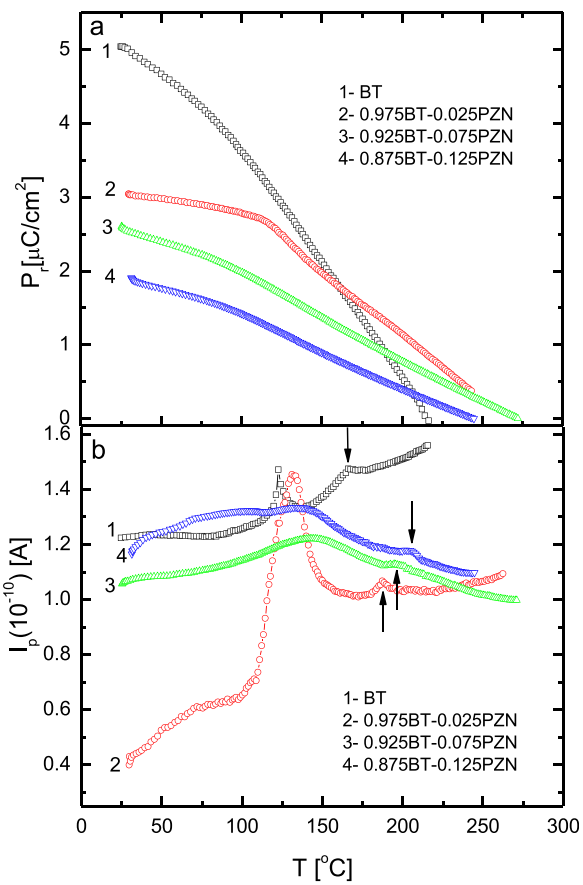

FIG. 7. Temperature dependence of the remnant polarization (a) and pyroelectric current (b) of (1-x)BT-xPZN ceramics. The arrow indicates an anomaly associated with the existence of polar regions.

There are two possible reasons why the dielectric and ferroelectric properties of BT tend to deteriorate after PZN incorporation. The first reason is associated with a change (decrease) in the dipole-dipole interaction. The replacement of Ba^{2+} ions by Pb^{2+} and Ti^{4+} ions by $(Zn,Nb)^{4+}$ causes the material disordering to be enhanced, leading to a disturbance of the long-range ferroelectric state of BT. On the other hand, the Pb^{2+} cation is smaller in size (1.49 Å) than Ba^{2+} (1.61 Å), which gives rise to compressive stress and a decrease in the lattice parameters upon substitution. Besides, distortion ("tetragonality") of the unit cell can be reduced as well. As a result, the dielectric and ferroelectric properties are expected to deteriorate. However, the $(Zn,Nb)^{4+}$ cation is larger (0.85 Å) than Ti^{4+} (0.74 Å), which generates tensile stress and leads to an increase in the lattice parameters upon substitution. As a consequence, distortion of the unit cell will be enhanced and dielectric and ferroelectric properties are expected to improve. As the differences in the size between A-site ions are slightly larger (0.12 Å) than those between B-site ions (0.11 Å), the first tendency seems to prevail. Local chemical disordering (chemical segregation) could also occur upon substitution, producing chemically ordered regions and as a consequence inducing the polar regions. Another reason why the dielectric/ferroelectric properties deteriorate is the change in the grain morphology. Movements of domain walls are relatively difficult when the grain size is non-uniform with some amount of pores (as for our BT-PZN system), which could lead to a decrease in electric permittivity and polarization. Moreover, non-uniform grains generate more internal stress, impeding the movements of the domain walls and reducing electric permittivity and polarization. Due to the difference in the ion size between Ba^{2+} and Pb^{2+} and Ti^{4+} and $(Zn,Nb)^{4+}$, it is reasonable to expect local elastic fields. As B-site substitution is not isovalent, a charge imbalance can occur in BT. A cation vacancy can be created (as shown by Raman analyses) to compensate for this imbalance, and local electric fields will be generated. As a result, polar regions will emerge, responsible for increased frequency dispersion and relaxor-type behavior.

On the other hand, substitution of Pb^{2+} for Ba^{2+} and $(Zn,Nb)^{4+}$ for Ti^{4+} can induce a stronger covalence (particularly the first substitution) due to the difference in electronegativity (1.8 vs. 0.9 and 1.6 vs. 1.5, respectively), which in turn may lead to improved ferroelectric properties. The nature of the Ba-O bond is purely ionic, whereas the nature of the Pb-O bond is covalent.[21] Indeed, the lone electron pair of Pb^{2+} hybridizes with oxygen's depleted p-orbitals, causing the formation of a metal-oxygen-metal (B-O-A) bond. This bonding changes the distortion of the TiO_6 octahedrons in the [001] direction. A change in distortion in the [001] direction is expected to mainly influence the vibrational

mode associated with the Ti-O bond. In fact, the Ti-O mode at about 270 cm^{-1} shifts to lower frequencies, which suggests a change (decrease) in distortion along the c-axis, which is corroborated by the X-ray data. Competition between these two effects: the increase in the covalent character of a chemical bond upon Pb^{2+} substitution and ionic size effects can lead to deterioration of the dielectric and ferroelectric properties of the BT-PZN system.

It is worth mentioning that BT-PZN is quite different from the BT-PMN system. In our opinion, the main reason is completely different nature of PZN and PMN materials. Namely, the latter is the relaxor exhibiting phase transition from the cubic phase to the rhombohedral one at about 140 °C (it means very close to pure BT), while the former is the canonical relaxor not undergoing any structural phase transition with the maximum of electric permittivity at about 5 °C. The close T_c values for BT and PZN cause the temperature of phase transitions slightly change with the increasing PZN content. One can see from Fig. 4 that at around 135 °C, always a maximum of electric permittivity appears that probably corresponds to the "main transition point". This may indicate that disorder in a dipole arrangement, the subsystem of BT-PZN does not change dramatically with an increase in the PZN content. Dynamics of this disordered subsystem nicely evolve into the relaxor-like behavior.

IV. CONCLUSIONS

New low-lead BT-PZN ceramics with a high relative density and excellent mechanical properties were obtained via the SPS technique. These ceramics have a pure perovskite structure with no secondary impurity. The effects of PZN incorporation into BT on the structural, thermal Raman, dielectric, and ferroelectric behaviors of these ceramics were investigated, showing that this incorporation has a major effect on the analyzed properties, leading to a shift of phase transformations, an increase in frequency dispersion, and deterioration of dielectric and ferroelectric properties. The results suggest that BT doping with PZN results in a material with strong dielectric dispersion in a wide temperature range, leading to almost relaxor behavior. It may be said that this behavior is similar to that observed for the BT-PMN system.[14] It appears that these effects are due to an increase in the covalent character of the A-O bond upon Pb^{2+} addition and due to ionic size differences and that the latter effect tends to prevail. Obviously, the BT-PZN system is a good choice as a low-lead electronic material.

ACKNOWLEDGMENTS

The present work was supported by the NCN project (No. 2012/05/B/ST5/00371).

[1]A. J. Moulson and J. M. Herbert, *Electroceramics* (Chapman and Hall, London, 1990).
[2]G. H. Hertling, "Ferroelectric ceramics: History and technology," J. Am. Ceram. Soc. **82**, 797–918 (1999).
[3]L. E. Cross, "Relaxor ferroelectrics," Ferroelectrics **76**, 241–267 (1987).
[4]F. Jona and G. Shirane, *Ferroelectric Crystals* (Pergamon Press, Oxford, London, New York, 1962).
[5]M. E. Lines and A. M. Glass, *Principles and Applications of Ferroelectrics and Related Materials* (Clarendon, Oxford, 1977).
[6]A. Ziębińska, D. Rytz, K. Szot, M. Górny, and K. Roleder, "Birefringence above Tc in single crystals of barium titanate," J. Phys. Condens. Matter **20**(1–5), 142202 (2008).
[7]J.-H. Ko, T. H. Kim, K. Roleder, D. Rytz, and S. Kojima, "Precursor dynamics in the ferroelectric phase transition of barium titanate single crystals studied by Brillouin light scattering," Phys. Rev. B **84**(1–6), 094111 (2011).
[8]A. Bussmann-Holder, H. Beige, and G. Volkel, "Precursor effects, broken local symmetry, and coexistence of order-disorder and displacive dynamics in perovskite ferroelectrics," Phys. Rev. B **79**(1–6), 184111 (2009).
[9]A. A. Bokov and Z.-G. Ye, "Recent progress in relaxor ferroelectrics with perovskite structure," J. Mater. Sci. **41**, 31 (2006).
[10]M. L. Mulvihill, L. E. Cross, W. Cao, and K. Uchino, "Domain-related phase transition-like behavior in lead zinc niobate relaxor ferroelectric single crystals," J. Am. Ceram. Soc. **80**, 1462–1468 (1997).
[11]A. Lebon, M. El Marssi, R. Farhi, H. Dammak, and G. Calvarin, "Translational and orientational order in lead zinc niobate: An optical and Raman study," J. Appl. Phys. **89**, 3947–3954 (2001).
[12]A. C. Larson and R. B. Von Dreele, Los Alamos National Laboratory Report No. LAUR 86–748 (2004).
[13]B. H. Toby, "EXPGUI, a graphical user interface for GSAS," J. Appl. Cryst. **34**, 210–213 (2001).
[14]J. Suchanicz, K. Świerczek, E. Nogas-Ćwikiel, K. Konieczny, and D. Sitko, "$PbMg_{1/3}Nb_{2/3}O_3$-doping effects on structural, thermal, Raman, dielectric and ferroelectric properties of $BaTiO_3$ ceramics," J. Eur. Ceram. Soc. **35**, 1777–1783 (2015).
[15]M. S. Jang, M. Takashige, S. Kojima, and T. Nakamura, "Oblique phonons with special concern to the soft phonon in tetragonal $BaTiO_3$," J. Phys. Soc. Jpn. **52**, 1025–1032 (1983).
[16]R. Farhi, M. E. Marssi, A. Simon, and J. Ravez, "A Raman and dielectric study of ferroelectric ceramics," Eur. Phys. J. B **9**, 99–604 (1999).
[17]S. Miao, J. Pokorny, U. M. Pasha, O. P. Thakur, D. C. Sinclair, and I. M. Reaney, J. Appl. Phys. **106**(1–6), 114111 (2009).
[18]P. E. Janolin, B. Dkhil, P. Bouvier, J. Kreisel, and P. A. Thomas, "Pressure instabilities up to 46 GPa in the relaxor ferroelectric $PbZn_{1/3}Nb_{2/3}O_3$," Phys. Rev. B **73**(1–9), 094128 (2006).
[19]J. Kreisel, A. M. Glazer, G. O. Jones, P. A. Thomas, P. A. Abello, and G. Lucazeau, "An X-ray diffraction and Raman spectroscopy investigation of A-site substituted perovskite compounds: The $(Na_{1-x}K_x)_{0.5}Bi_{0.5}TiO_3$ ($0 < x < 1$) solid solution," J. Phys. Condens. Matter **12**, 3267–3280 (2000).
[20]B. Zalar, V. V. Laguta, and R. Blinc, "NMR Evidence for the coexistence of order-disorder and displacive components in barium titanate," Phys. Rev. Lett. **90**, 037601 (2003).
[21]R. E. Cohen, Nature **358**, 136–140 (1992).